Fabrication of temperature- and pH-sensitive liquid-crystal droplets with PNIPAM-*b*-LCP and SDS coatings by microfluidics

Yong-Dae Jung, Mashooq Khan and Soo-Young Park[*]

School of Applied Chemical Engineering, Kyungpook National University, 1370 Sangyuk-dong, Buk-gu, Daegu 702-701, Korea

[*]To whom correspondence should be addressed.

Tel.: +82-53-950-5630; fax: +82-53-950-6623; e-mail: psy@knu.ac.kr

Abstract: Dual responsive (temperature and pH) 4-cyano-4′-pentylbiphenyl (5CB) droplets were fabricated by coating with PNIPAM-*b*-LCP (PNIPAM: poly(*N*-isopropylacrylamide); LCP: poly(4-cyanobiphenyl-4′-oxyundecylacrylate)) and sodium dodecyl sulfate (SDS) using a microfluidic method, and were tested for protein detection. The PNIPAM-*b*-LCP/SDS-functionalized 5CB droplets were effective in detecting proteins in water through a radial-to-bipolar (R–B) orientational change, with detection limits of 0.95, 1.1, 0.12, and 0.07 μM for bovine serum albumin (BSA), lysozyme (LYZ), hemoglobin (Hb), and chymotrypsinogen (ChTg), respectively. The R–B change of the 5CB droplet occurred above the lower critical solution temperature (LCST) of PNIPAM and at pH values below the pI values of the tested proteins, and was reversible by heating/cooling at the LCST of PNIPAM. These sensitive 5CB droplets are simple to prepare, cost-effective, easy detection, and re-usable (by temperature control) for protein detection. Further, it can be applied to a biosensor after employing the selective units such as aptamers, antibodies, single-stranded DNA, proteins, peptides, and aptamer-binding RNA on the droplet.

Keywords: Protein, Biosensor, Liquid-Crystal, SDS, block copolymer

Introduction: The detection and characterization of specific proteins is used extensively as the basis for the molecular screening of diseases, food-borne toxins, narcotics in blood, and novel drugs.[1]   Established methods for detecting and characterizing proteins mostly involve surface immobilization of the protein of interest onto a solid substrate;[2-4] liquid crystals (LCs), as one example, have become one of the most important tools in biological sensors.[5-8] Some unique properties possessed by LCs include high sensitivity of LC orientations to minute changes on the surface, liquid-like mobility that can amplify LC responses within tens of milliseconds, high birefringence, and orientational changes of the LCs that can be easily observed under a polarized optical microscope (POM) with crossed polarizers.   The ability of LCs to transduce and amplify molecular events at an LC/water interface into optical images visible to the naked eye has been successfully reported.[9, 10] LC-based sensors are simple, label-free, and allow real-time reporting of various biological events[1, 11] such as the enzymatic hydrolysis of phospholipids, specific phospholipid-protein binding, and DNA hybridization.[6, 12-14] The anchoring of LCs at the LC/water interface can be coupled with reorientations of the LCs as a response to the presence of surfactants,[5, 6, 12] lipids,[13] proteins,[14, 15] and polymers[16-19] adsorbed at the LC/water interface. When using "smart" (or stimuli-responsive) adsorbed polymers, the LC orientations become sensitive to environmental stimuli in the aqueous phase.   Smart polymers that respond to environmental stimuli such as pH,[19, 20] temperature,[21] ionic strength,[22] electrical potential,[23] magnetic field,[24]   and light[25] have attracted much interest for applications such as biosensors, protein purification,[26] and tissue engineering.   Recently, we reported the preparation of a pH-responsive and room temperature–stable nematic 4-cyano-4´-pentylbiphenyl (5CB) LC/water interface functionalized with PAA-*b*-LCP (PAA: poly(acrylic acid); LCP: poly(4-cyanobiphenyl-4-oxyundecylacrylate)), in which PAA and LCP chains were in water and 5CB, respectively. This functionalized interface adopts either a flat surface when using a transmission electron

microscopy (TEM) grid cell[10] or a spherical surface when using the LC droplets produced by a microfluidic method.[27] We found that PAA-*b*-LCP conferred pH-dependent anchoring to the director orientation of 5CB at the 5CB/water interface by a change in the charge state of the PAA block in water. PAA, a weak polyelectrolyte, was modified from the almost uncharged state to the fully charged state by a pH change. This charged state of the PAA chains on the surface of micro-sized LC droplets affected the director configuration of the LC droplet on exposure to different pH values. Its responsiveness to pH was confirmed by the distinct change in the director configuration of LC ordering in the droplet using POM analysis under crossed polarizers.

The temperature-responsive poly(*N*-isopropylacrylamide) (PNIPAM) is also one of the most extensively studied smart polymers owing to its reversibility and fast response. In an aqueous environment, PNIPAM undergoes a solubility switch at its lower critical solution temperature (LCST) of 32 °C; PNIPAM chains are swollen, highly hydrated, and hydrophilic below its LCST, and become collapsed and more hydrophobic above its LCST because of an entropically driven dissociation of water molecules.[28] In the literature, protein interactions with PNIPAM-immobilized surfaces have been studied by monitoring the amount of adsorbed protein as a function of temperature.[29-31] The general observation was that the PNIPAM surface adsorbed significantly more proteins above its LCST than below it. Ratner et al. studied protein adsorption and biological recognizability on plasma-polymerized NIPAM surfaces above and below the LCST of PNIPAM. The reversible adsorption/desorption and binding strength of proteins have also been discussed in a number of studies.[32-34]

In this study, we successfully prepared poly(*N*-isopropylacrylamide)-*b*-poly(4-cyanobiphenyl-4′-oxyundecylacrylate) (PNIPAM-*b*-LCP)-coated 5CB (5CB$_{PNIPAM}$) droplets

incorporating an anionic surfactant, sodium dodecyl sulfate (SDS), by a microfluidic method, and tested their thermal and pH responses as well as protein adsorption on the droplet surface. The change in the director profile due to protein adsorption on the $5CB_{PNIPAM}$ droplets was examined by POM observations under crossed polarizers to assess the utility of the $5CB_{PNIPAM}$ droplets toward protein-detection sensing applications. Particularly, the effects of hydrophilicity (or hydrophobicity) of PNIPAM (controlled by temperature) and pH of the medium on the direct configuration of the $5CB_{PNIPAM}$ droplets through protein adsorption were studied in order to find the origins of this configurational change. Our simple and inexpensive technique is anticipated to provide a fundamental understanding of protein interactions on the dual (thermal and pH)-responsive PNIPAM/SDS surfaces that will help to guide the development of PNIPAM-based materials for protein detection and other biological applications.

Experimental

Materials: 4-Cyano-4'-pentylbiphenyl (5CB, Merck, Japan), *n*-octadecyltrichlorosilane (OTS, Sigma-Aldrich), methanol (Sigma-Aldrich), buffer solutions (pH = 2–12, Samchun Chemicals Korea), dichloromethane (DCM, Aldrich), poly(dimethylsiloxane) (PDMS) kit (Sylgard 184, Dow Corning, USA, containing the pre-polymer and a cross-linker), and sodium dodecyl sulfate (SDS) were used as received. Lysozyme (LYZ) was purchased from MP Biomedicals and bovine serum albumin (BSA), hemoglobin (Hb), and chymotrypsinogen (ChTg) were supplied by Sigma-Aldrich. Milli-Q water (resistivity higher than 18.2 MΩ cm) was used throughout the experiments. Glass microscope slides (S9213, Matsunami, Japan, $76 \times 52 \times 1.3$ mm^3) were cleaned with a hot piranha solution (H_2O_2 (35%):H_2SO_4 (98%) = 1:1 (v/v)) for 30 min, washed with water, and finally dried under a nitrogen flow (*caution*: piranha solution is extremely corrosive and must be handled carefully).

Synthesis of PNIPAM-*b*-LCP: PNIPAM-*b*-LCP was synthesized using a method reported elsewhere.[18] The molecular weight was PNIPAM(43.5K)-*b*-LCP(10.5K) with a polydispersity index (M_w/M_n) of 1.22. Scheme 1 outlines the synthesis of PNIPAM(43.5K)-*b*-LCP(10.5K) commencing with the polymerization of *N*-isopropylacrylamide (NIPAM) using a chain-transfer agent (CTA) and azobisisobutyronitrile (AIBN) as a radical initiator. Figure S1 (see Supplementary Information, SI) shows the FT-IR and ^{1}H NMR spectra of the synthesized PNIPAM(43.5K)-*b*-LCP(10.5K).

Device fabrication: For the fabrication of the microfluidic flow-focusing devices, PDMS was prepared by mixing the pre-polymer and cross-linker thoroughly at the recommended ratio of 10:1 (w/w) and degassing the mixture for 40 min in a desiccator to remove the remaining air bubbles. The final mixture was poured onto a structured silicon wafer mold and cured inside an oven at 65 °C for 4 h before removing it from the mold. This patterned piece of PDMS was bonded to a pre-cleaned glass microscope slide using a short oxygen plasma treatment (46 s duration, Femto Science Inc., Korea). Figure 1 shows a schematic diagram of the microchip and dimensions of the microfluidics channel. The width of the inlet channels, the orifice width and length, and the width and height of the outlet channel were 110, 40, 40, 160, and 40 μm, respectively, and the depth of the channels throughout was 100 μm. The channel walls and chip assembly were made hydrophilic by oxygen plasma treatment. The channel was filled with water until the chip was used.

Production and analysis of the LC droplets: The microfluidic chip was mounted under an inverted biological microscope (Samwon NSI-100, South Korea). The liquid samples were supplied to the microfluidic device through flexible plastic tubing (Norton, USA, I.D. 0.51 mm, O.D. 1.52 mm) attached to precision syringes (SGE Analytical Science, Australia)

operated by digitally controlled syringe pumps (KD Scientific, KDS 100 series, USA). The flow of fluids to the microfluidic channels was controlled with two independent syringe pumps. The formation of the on-chip droplets was imaged with a STC-TC83USB-AS camera (SenTech, Japan) attached to an inverted microscope. The droplets were observed under a POM (Samwon LSP-13, South Korea) with crossed polarizers. The dispersed LC phase was slowly injected into the middle inlet, and the aqueous continuous phase containing 0.1 wt% PNIPAM-*b*-LCP and 0.1 wt% SDS was injected into the other inlets in a direction perpendicular to the dispersed phase (Figure 1). Both the phases met at the junction and droplet formation took place when the fluids crossed the neck of the channel. The $5CB_{PNIPAM}$ droplets were extracted from the microchip and collected in a $14 \times 8 \times 2.5$ mm^3 storage reservoir, which was made by gluing a thin silicon rubber sheet onto the glass slide.

Results and Discussion

Generation of PNIPAM-*b*-LCP-coated LC droplets: Figure 1b shows the synthesized $5CB_{PNIPAM}$ droplets with a mean diameter of 35 ± 1.3 μm. The PNIPAM-*b*-LCP acted as a surfactant because of its amphiphilic nature;[34] the LCP block functioned to strongly anchor the incorporated 5CBs by penetrating into the 5CB droplet (due to compatibility between the LCs and mesogenic groups of LCP), while the presence of the hydrophilic PNIPAM block on the surface of the 5CB droplet was thought to prevent the coalescence of the 5CB droplets. Additionally, the added SDS coating on the 5CB droplet could induce negative charges on the 5CB droplets. These uniform $5CB_{PNIPAM}$ droplets may present a well-defined model system for the investigation of the interactions between proteins and thermo-responsive PNIPAM chains on the surface of the 5CB droplet.

Internal orientations of the 5CB droplet were next analyzed by POM under crossed polarizers. The 5CB droplets synthesized without any coating are known to have a bipolar

configuration.[20, 27] Figure 2a shows a POM image of the 5CB$_{PNIPAM}$ droplets without SDS functionalization under crossed polarizers. A clear bipolar configuration was observed, indicating that the PNIPAM-*b*-LCP coating on the 5CB droplets did not affect the direct orientation of 5CB in the droplet. This observation might be due to the neutrality of the charge state of the PNIPAM chains. Studies on the PAA-b-LCP-coated 5CB (5CB$_{PAA}$) droplets reported that the configurational orientation of 5CB was controlled by the charge state at the interface.[35, 36] A radial orientation is preferred for the detection of protein adsorption through an LC orientational change of the 5CB droplet, because protein adsorption causes a bipolar orientation (which will be discussed later) and a radial-to-bipolar (R–B) orientational change due to protein adsorption can be optically observed using POM under crossed polarizers. To achieve a radial orientation in the 5CB$_{PNIPAM}$ droplet, SDS was used together with PNIPAM-*b*-LCP in the continuous phase. SDS is an anionic surfactant typically used to induce the perpendicular (radial) orientation of 5CB at the LC/water interface caused by the penetration of the alkyl chains of SDS into the 5CB. Figure 2b shows a POM image of the 5CB$_{PNIPAM}$ droplets functionalized with 0.1 wt% SDS. The 5CB$_{PNIPAM}$ droplets showed a Maltese cross formation, suggesting that a perpendicular (radial) orientation of 5CB against the LC/water interface was induced by the SDS addition. This radial orientation did not change with pH of the solution (which will be discussed with Figure 4). Thus, this PNIPAM-*b*-LCP/SDS-functionalized 5CB droplet had a reference radial orientation and could be used for protein detection.

Temperature effect on protein adsorption: The model protein LSZ was used to study the effect of temperature on protein adsorption on the 5CB$_{PNIPAM}$ droplets. The 5CB$_{PNIPAM}$ droplets were collected from the main micro-channel connecting into the reservoir, which contained a 0.1 wt% LSZ solution at pH 11. The choice of pH 11 will be discussed with

Figure 4. Figure 3a shows the POM images of the 5CB_{PNIPAM} droplet in water without proteins at different temperatures. The reservoir with the 5CB_{PNIPAM} droplets was placed on a heating glass (CU-201, Live Cell Instruments) and slowly heated from 30 to 40 °C at a rate of 0.3 °C/min. The initial radial configuration of the 5CB_{PNIPAM} droplet below LCST of PNIPAM (32 °C) did not change with heating above the LCST. This result strongly suggests that the expansion and shrinkage of the PNIPAM chains did not affect the direct configuration of the 5CB_{PNIPAM} droplet. Figures 3b and c show the POM images of the 5CB_{PNIPAM} droplets in the reservoir containing 0.1 wt% LSZ during heating and cooling, respectively. During heating (Figure 3b), a switch from radial to bipolar configuration was observed at the LCST of PNIPAM. This result indicates that shrinkage of the PNIPAM chains above its LSCT caused the adsorption of LSZ on the 5CB_{PNIPAM} droplets. During cooling (Figure 3c), a switch from bipolar to radial configuration was observed at the LCST of PNIPAM, indicating that protein adsorption and desorption processes were reversible. Thus, protein adsorption and desorption could be controlled by temperature as shown in the schematic of Figure 3d; PNIPAM chains are swollen, highly hydrated, and hydrophilic below their LCST, and collapse and become more hydrophobic above their LCST because of the entropically driven dissociation of water molecules. The swollen hydrophilic PNIPAM chains below its LCST prevented protein adsorption; however, the collapsed PNIPAM chains above its LCST could induce protein adsorption on the LC droplets. The reasons for protein adsorption may be the result of electrostatic interactions, hydrogen bonding, hydrophobic interactions, etc. PNIPAM chains above its LCST are hydrophobic and the SDS present on the 5CB droplets has negative charges; accordingly, both electrostatic and hydrophobic interactions should be considered when studying the origins of protein adsorption on the 5CB_{PNIPAM} droplets.

pH effect on protein adsorption: To study the origin of protein adsorption on the $5CB_{PNIPAM}$ droplets, an investigation of protein adsorption with proteins having different isoelectric points (pIs) is important for determining the role of the electrostatic interaction, as the charge state of the protein is strongly dependent on its pI, allowing for the study of protein adsorption by electrostatic interactions in relation to its pH dependency. BSA, Hb, ChTg, and LYZ were tested with the $5CB_{PNIPAM-SDS}$ droplets. The pIs of BSA, Hb, ChTg, and LYZ are 5.3, 6.8, 8.9 and 11.35, respectively.[15] Proteins can be denatured under a range of physical conditions, including high temperature, very low or high pH, and very high pressure;[37] however, the purpose of this study was to detect proteins, even though they might be denatured at pHs lower and higher than physiological conditions. Figure 4 shows POM images of the $5CB_{PNIPAM}$ droplets under crossed polarizers with 0.1 mg/mL protein solutions at different pHs above and below the LCST of PNIPAM.   The initial configuration of the $5CB_{PNIPAM}$ droplets without proteins was radial, as previously mentioned.   The POM images of the $5CB_{PNIPAM}$ droplets below LCST showed an unchanged radial orientation regardless of pH for all tested proteins, even though those above LCST were dependent on pH in such a way that bipolar (through a R–B change) and unchanged radial orientations were observed below and above the pI, respectively. The R–B change above LCST might be due to protein adsorption through hydrophobic interactions between the collapsed PNIPAM chains and proteins. Another factor to be considered for protein adsorption on the $5CB_{PNIPAM}$ droplets is the electrostatic interactions between the coated anionic SDS and proteins, which can be attractive or repulsive at pHs below and above their pIs, respectively.   The fact that the R–B change occurred only at pHs below the pIs of the proteins indicates that the attractive force between SDS and the protein is necessary for inducing the R–B transition (see Figure 3d). However, as discussed, protein adsorption on the PNIPAM chain did not occur below the LCST of PNIPAM, even at pHs below the protein pIs, because the swollen PNIPAM chains

prevented protein adsorption, thus limiting the electrostatic interaction force due to long separation between SDS and proteins. Thus, the manipulation of PNIPAM chains and SDS surfactants using temperature and pH, respectively, on the 5CB$_{PNIPAM}$ droplets can control protein adsorption. This dual response of the 5CB$_{PNIPAM}$ droplets can be beneficial for their use as biosensors since temperature-controlled reversible protein adsorption/desorption permits their reuse, and selective protein adsorption by pH modification can be easily controlled.

Sensitivity of the 5CB$_{PNIPAM}$ droplets: The sensitivity of protein detection can be defined as the lowest protein concentration at which orientational configurations of the 5CB$_{PNIPAM}$ droplets are changed by protein adsorption. Figure 5 shows POM images of the 5CB$_{PNIPAM}$ droplets under crossed polarizers after injecting 0.1 mg/mL BSA, Hb, ChTg, and LYZ solutions at 35 °C (above LCST) and below the pIs as a function of protein concentration. The pHs of the 5CB$_{PNIPAM}$ droplets were 5, 6, 8, and 11 for BSA, Hb, ChTg, and LYZ, respectively. R−B changes were observed at concentrations higher than 0.95, 0.12, 0.07, and 1.1, μM for BSA, Hb, ChTg, and LYZ, respectively. This low detection limit suggests that 5CB$_{PNIPAM}$ droplets can be applied to biosensors if selective functional groups such as antibodies and aptamers are employed. These results also demonstrate the utility of 5CB$_{PNIPAM}$ droplets for detection of small amounts of proteins by a simple microscopic method through the naked eye.

Conclusion: The as-synthesized 5CB$_{PNIPAM}$ droplets were found to be effective in detecting proteins in water through inducing an R−B change caused by the adsorption of proteins on the PNIPAM chains of the 5CB droplet above the LCST of PNIPAM and below the tested protein's pI. The R−B transition through protein adsorption was reversible at the LCST of PNIPAM. The detection limits for BSA, LYZ, Hb, and ChTg were 0.95, 1.1, 0.12, and 0.07

μM, respectively. This simple, convenient, and re-usable (by temperature control) protein detection system can be used as a biosensor after employing the selective units on the surface. These studies on the temperature and pH-dependent protein adsorption onto $5CB_{PNIPAM}$ droplets will facilitate the understanding of protein interactions on the thermo-responsive PNIPAM surfaces that may guide the use of PNIPAM for biosensors and other biological applications.

References:

1.   D. Hartono, C.-Y. Xue, K.-L. Yang and L.-Y. L. Yung, *Advanced Functional Materials*, 2009, **19**, 3574-3579.
2.   K. Nakanishi, T. Sakiyama, Y. Kumada, K. Imamura and H. Imanaka, *Current Proteomics*, 2008, **5**, 161-175.
3.   Y. Kumada, C. Zhao, R. Ishimura, H. Imanaka, K. Imamura and K. Nakanishi, *Journal of Biotechnology*, 2007, **128**, 354-361.
4.   P. Billsten, M. Wahlgren, T. Arnebrant, J. McGuire and H. Elwing, *Journal of Colloid and Interface Science*, 1995, **175**, 77-82.
5.   Y.-Y. Luk and N. L. Abbott, *Curr. Opin. Colloid Interface Sci.*, 2002, **7**, 267-275.
6.   A. D. Price and D. K. Schwartz, *Journal of the American Chemical Society*, 2008, **130**, 8188-8194.
7.   D. Hartono, X. Bi, K.-L. Yang and L.-Y. L. Yung, *Advanced Functional Materials*, 2008, **18**, 2938-2945.
8.   S. J. Woltman, G. D. Jay and G. P. Crawford, *Nature Material*, 2007, **6**, 929-938.
9.   X. Bi, D. Hartono and K.-L. Yang, *Adv. Func. Mater.*, 2009, **19**, 3760-3765.
10.   D.-Y. Lee, J.-M. Seo, W. Khan, J. A. Kornfield, Z. Kurji and S.-Y. Park, *Soft Matter*, 2010, **6**, 1964-1970.
11.   A. R. Wise, J. A. Nye and J. T. Groves, *ChemPhysChem*, 2008, **9**, 1688-1692.
12.   J. M. Brake, A. D. Mezera and N. L. Abbott, *Langmuir*, 2003, **19**, 6436-6442.
13.   J. M. Brake, M. K. Daschner, Y. Y. Luk and N. L. Abbott, *Science*, 2003, **302**, 2094-2097.
14.   D. Hartono, W. J. Qin, K.-L. Yang and L.-Y. L. Yung, *Biomaterials*, 2009, **30**, 843-849.
15.   J. M. Seo, W. Khan and S.-Y. Park, *Soft Matter*, 2012, **8**, 198-203.
16.   M. I. Kinsinger, M. E. Buck, N. L. Abbot and D. M. Lynn, *Langmuir*, 2010, **26** 10234–10242.
17.   M. I. Kinsinger, M. E. Buck, M.-V. Meli, N. L. Abbott and D. M. Lynn, *Journal of Colloid and Interface Science*, 2010, **341**, 124-135.
18.   W. Khan, J.-M. Seo and S. Y. Park, *Soft Matter*, 2011, **7**, 780-787.
19.   D. Y. Lee, J. M. Seo, W. Khan, J. A. Kornfield, Z. Kurjib and S. Y. Park, *Soft Matter*, 2010, **6**, 1964-1970.
20.   J. Kim, M. Khan and S.-Y. Park, *ACS Applied Materials & Interfaces*, 2013, **5**, 13135-13139.
21.   L. F. Gudeman and N. A. Peppas, *J Membr Sci.*, 1995, **107**, 239-248.
22.   J. F. Hester, S. C. Olugebefola and A. M. Mayes, *Journal of Membrane Science*, 2002, **208**, 375-388.
23.   L. Ying, P. Wang, E. T. Kang and K. G. Neoh, *Macromolecules*, 2001, **35**, 673-679.
24.   M. Orlov, I. Tokarev, A. Scholl, A. Doran and S. Minko, *Macromolecules*, 2007, **40**, 2086-2091.
25.   Q. Wei, J. Li, B. Qian, B. Fang and C. Zhao, *Journal of Membrane Science*, 2009, **337**, 266-273.
26.   Q. Shi, Y. Su, W. Zhao, C. Li, Y. Hu, Z. Jiang and S. Zhu, *Journal of Membrane Science*, 2008, **319**, 271-278.
27.   W. Khan, J. H. Choi, G. M. Kimb and S. Y. Park, *Lab Chip*, 2011, **11**, 3493-3498.
28.   H. G. Schild, *Progress in Polymer Science*, 1992, **17**, 163-249.
29.   E. C. Cho, Y. D. Kim and K. Cho, *Journal of Colloid and Interface Science*, 2005, **286**, 479-486.
30.   D. Cunliffe, C. de las Heras Alarcón, V. Peters, J. R. Smith and C. Alexander, *Langmuir*, 2003, **19**, 2888-2899.
31.   L. B. John, in *Proteins at Interfaces III State of the Art*, American Chemical Society, 2012, vol. 1120, ch. 12, pp. 277-300.
32.   D. Duracher, R. Veyret, A. Elaïssari and C. Pichot, *Polymer International*, 2004, **53**, 618-626.
33.   T. Taniguchi, D. Duracher, T. Delair, A. Elaïssari and C . Pichot, *Colloids and Surfaces B: Biointerfaces*, 2003, **29**, 53-65.
34.   H. Kawaguchi, K. Fujimoto and Y. Mizuhara, *Colloid Polym Sci*, 1992, **270**, 53-57.

35.   M. Khan and S.-Y. Park, *Analytical Chemistry*, 2013.
36.   R. J. Carlton, J. K. Gupta, C. L. Swift and N. L. Abbott, *Langmuir*, 2012, **28**, 31-36.
37.   D. Kishore, S. Kundu and A. M. Kayastha, *PLoS ONE*, 2012, **7**, e50380.
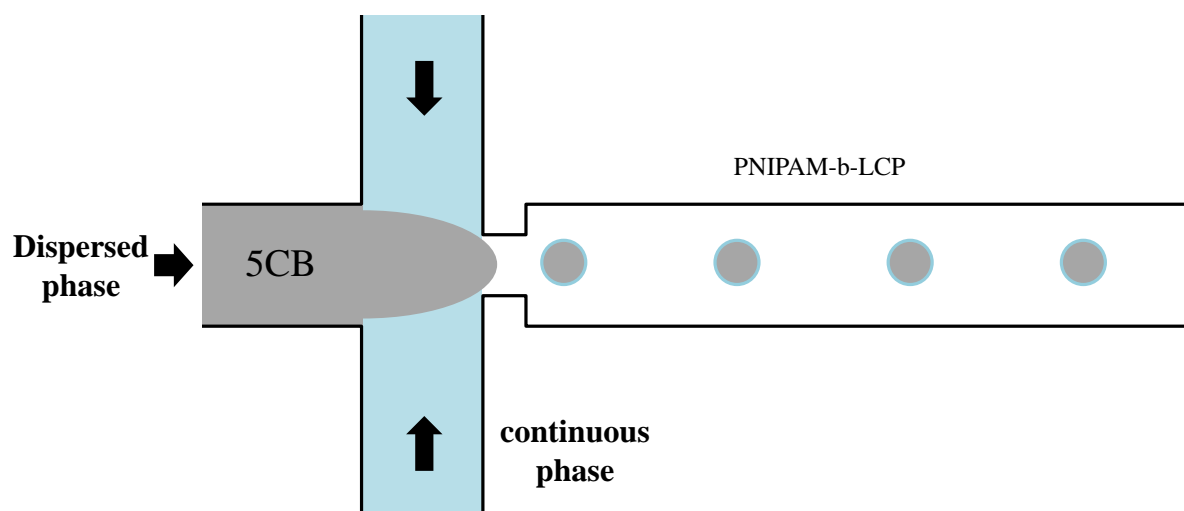
(a)
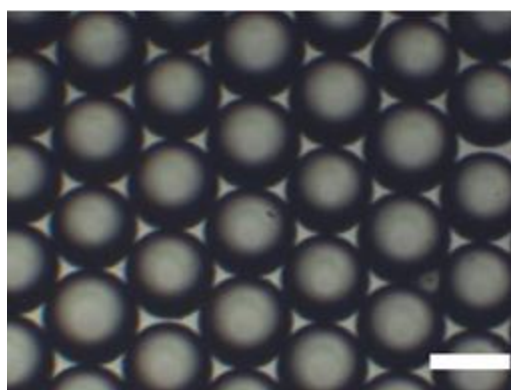
(b)

Figure 1. (a) Formation of monodisperse droplets in a microfluidic chip; the dispersed and continuous phases were 5CB and aqueous PNIPAM-*b*-LCP (0.1 wt%)/SDS (0.1 wt%), respectively. (b) Optical images of the produced $5CB_{PNIPAM}$ droplets; the scale bar shown is 35 μm.
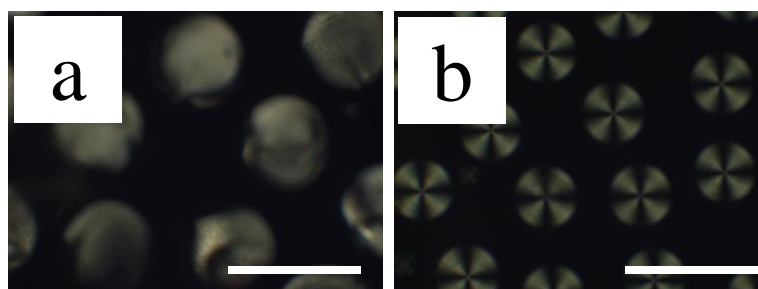
Figure 2. POM image (under crossed polarizers) of 5CB$_{PNIPAM}$ droplets in pure water (a) without and (b) with SDS coating. The scale bars represent 100 µm.
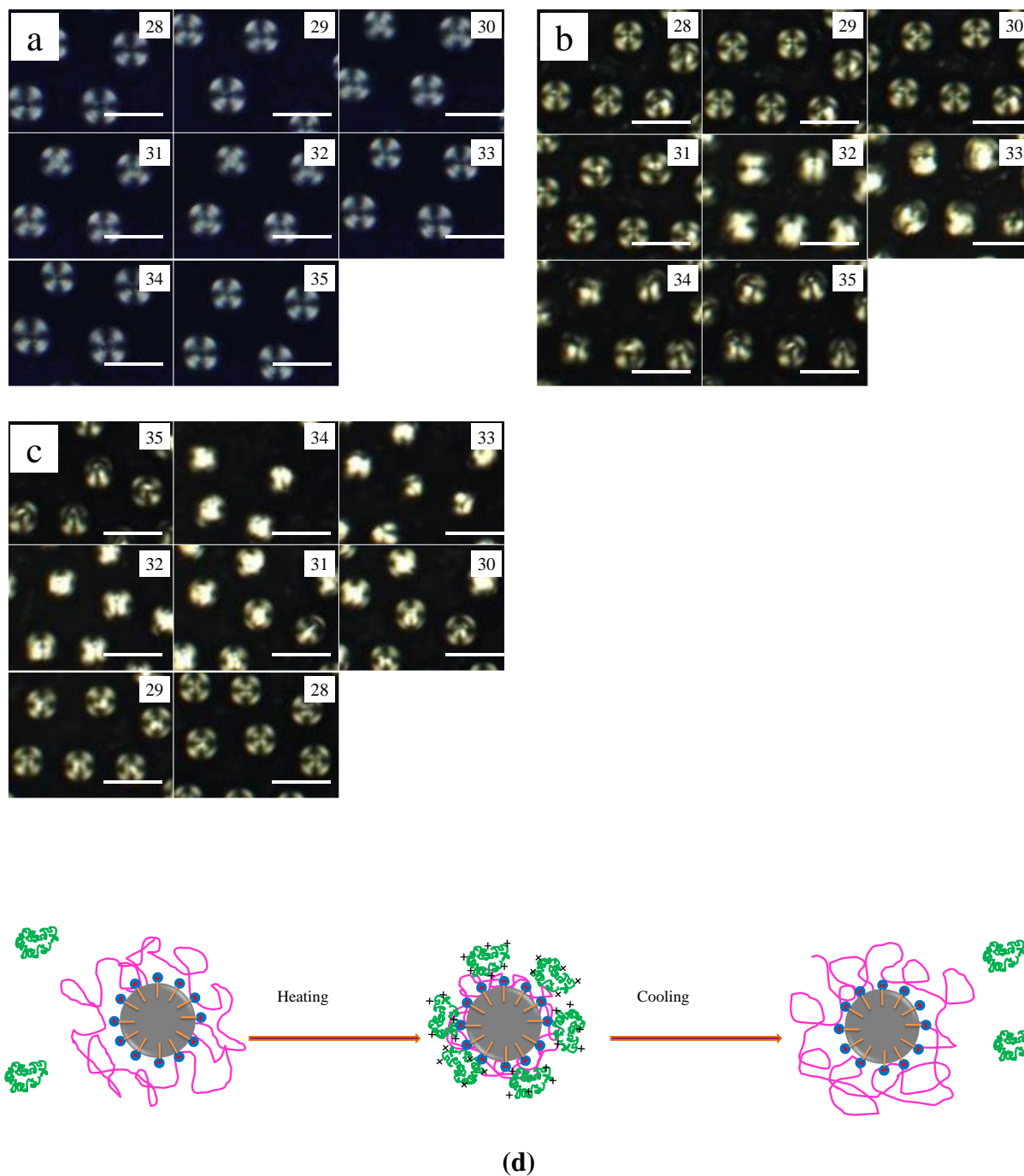
Figure 3. POM images of the 5CB$_{PNIPAM}$ droplets in aqueous solution under crossed polarizers (a) without and (b, c) with 0.1 wt% LSZ during (a, b) heating and (c) cooling of the reservoir (the numbers in the figures represent temperature (°C); the same 100 μm scale bar is applied to all images); (d) schematic of the reversible shrinking and expansion of the PNIPAM chains with the ultimate adsorption and desorption of LSZ during heating and cooling.
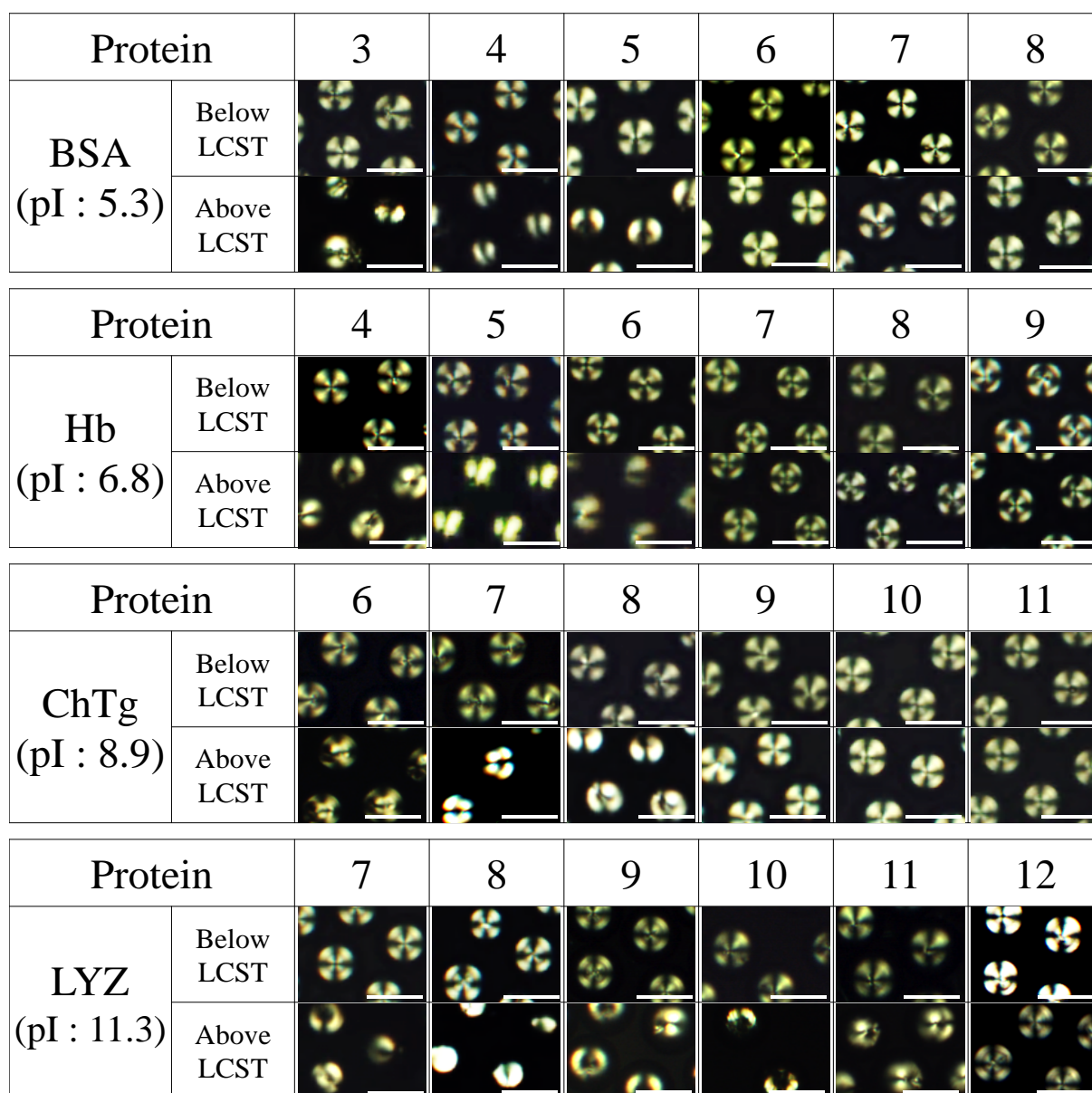
Figure 4. POM images (under crossed polarizers) of the 5CB$_{PNIPAM}$ droplets with 0.1 mg/mL protein solutions at different pHs above and below LCST (32 °C). The scale bars represent 100 μm.
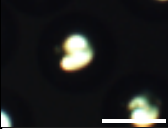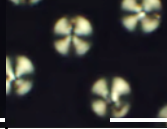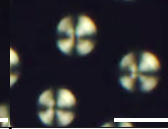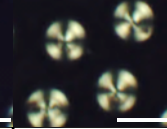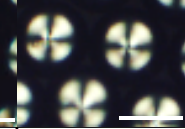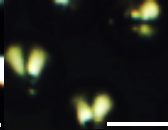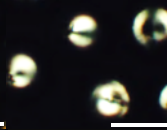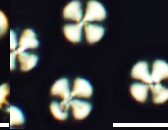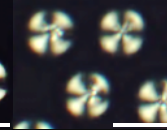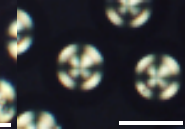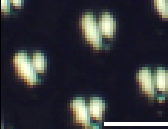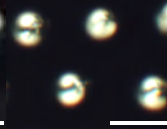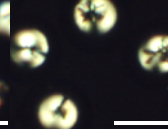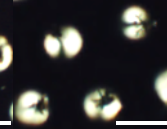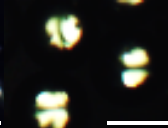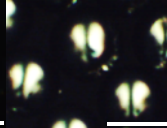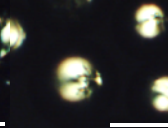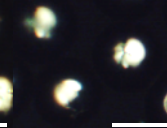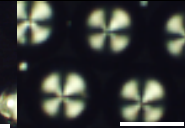
wt%	0.1	0.01	0.0075	0.005	0.0025	0.001
ChTg (pH8)						
	(39.1)	(3.91)	(2.93)	(1.95)	(0.98)	(0.39)
BSA (pH5)						
	(15.2)	(1.52)	(1.14)	(0.76)	(0.38)	(0.15)
LYZ (pH11)						
	(69.2)	(6.92)	(5.19)	(3.46)	(1.73)	(0.69)
Hb (pH6)						
	(15.5)	(1.55)	(1.16)	(0.78)	(0.39)	(0.15)

Figure 5. POM images of the 5CB$_{PNIPAM}$ droplets under crossed polarizers at different protein concentrations; the numbers in parentheses are the protein concentration in μM; the scale bar represents 100 μm and is applied to all images.
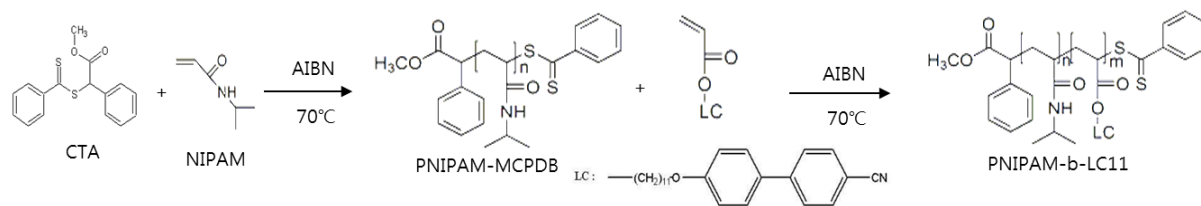
Scheme 1. Synthesis of PNIPAM-*b*-LCP